Harmonic Suppression in the Fourth Wire of a Three-Phase Four-Wire Shunt Active Power Filter

Miguel Ochoa-Giménez*, Aurelio García-Cerrada, Juan Luis Zamora-Macho
Institute for Research in technology (IIT), School of Engineering (ICAI) Comillas Pontifical University
Javier Roldán-Pérez, Norvento Enerxia

***Abstract*—Control of three-phase voltage source converters in Synchronous Reference Frames (SRF) is a well-know method with an intrinsic frequency adaptation capability and a simple design. However, the application of this method to the zero-sequence component of four-wire three-phase converters is not straight forward. As there is only one signal in the zero-sequence component, a quadrature signal is always created in order to have the two components of a space vector, similarly to the three-phase case using Park's Transformation. This paper presents an alternative control method based on multiple reference frames for tracking or rejecting periodic signals applied to the control of the zero-sequence current of a four-wire shunt active power filter. It is demonstrated that the proposed approach can be used without creating the quadrature signal of the error, whilst maintaining an intrinsic adaptation capability to grid-frequency variations. The main contributions of this paper are validated using a laboratory prototype.**

I. Introduction

Steady-state voltages and currents in electric power systems (balanced or unbalanced) consist of a fundamental component of 50 or 60 Hz plus harmonics with frequencies which are integer multiples of the fundamental one. Voltage and current harmonics in electric power systems produce additional power losses, equipment heating, fuse and breaker malfunction and torque pulsations in electrical motors. Harmonics are produced by non-linear devices such as AC-to-DC converters, arc furnaces, saturated transformers, etc. Meanwhile, distribution systems are inherently unbalanced because of untransposed distribution lines, unequally-loaded phases and unbalanced loads. Therefore, unwanted negative- and zero-sequence currents are often present. The negative sequence will cause excessive heating in machines and low-frequency ripples in rectifiers, and the zero-sequence currents cause not only excessive power losses in neutral lines, but also degrade the circuit protection [1].

Active power filters (APF) based on controlled Voltage Source Converters (VSC) are a flexible alternative to compensate current and voltage unbalance and harmonic disturbances [2]. Power flow in three-wire three-phase VSCs is often controlled using a Synchronous Reference Frame (SRF) tight to the grid frequency because Proportional-Integral (PI) controllers achieve zero steady-state error [3].

*Corresponding author: Miguel Ochoa, Comillas Pontifical University, Address: c/Santa Cruz de Marcenado, 26, Madrid, Spain, E-mail: Miguel.Ochoa@iit.upcomillas.es, Phone: +34 91 542 28 00, Fax: +34 91 542 31 76

The dq components of electrical magnitudes are DC quantities in steady state and can be controlled independently from the zero-sequence component which is rarely of interest. In four-wire systems, however, the zero-sequence component must be taken care of and it is treated as a single-phase system. However, harmonics are still seen as sinusoids in the SRF used and cannot be tackled so easily. Furthermore, unbalanced electrical variables also produce sinusoids in the d-q and in the zero-sequence components. Thus, harmonic control must be addressed for d, q and zero-sequence components in four-wire systems.

Harmonic control in power electronics has been addressed using, mainly, selective controllers ([4], [5],[6],[7]), repetitive controllers ([8], [9]) and multiple SRFs or MSRFs ([10]). The first and second alternatives can be readily applied to single-phase systems (such as the zero-sequence component) but their design is cumbersome and their adaptation to frequency variations require extra work. In the third approach, when applied to three-phase systems, Park's Transformation is applied several times to the three-phase magnitudes using, each time, the position of a reference frame which rotates with respect to the fundamental-frequency d-q reference frame with an angular speed related to a harmonic frequency. In this scenario, PI controllers can be designed independently for each harmonic once it is referred to the appropriate SRF because its d-q components are constant values in steady state. This procedure is very attractive from the design viewpoint and its intrinsic frequency adaptation capability, but has always been considered as cumbersome because many trigonometric functions have to be calculated in real-time. However, recently, an efficient implementation of this controller has been proposed [11].

The application of MSRFs to a single-phase system is typically carried out using a quadrature component of the error, which is artificially generated [12] but, in this paper, an alternative procedure will be proposed. Variations of the grid frequency will be addressed because in modern power systems, with a large penetration of renewable energy sources connected at the distribution level, and in micro-grids, the fundamental frequency of the electrical magnitudes might show larger variations [13] and over longer periods of time [14] than in conventional distribution systems. Experimental results of the proposed controller will be presented in the context of a four wire three-phase shunt active power filter used to balance the grid currents and to suppress harmonics produced by an unbalanced non-linear load. Since

the analysis and design of the control for the d and q current components is fully described in [11], this paper will focus on the zero-sequence component.

II. System Description and Zero-Sequence Model in a SRF

A four-wire shunt active power filter (Fig. 1) has been used to illustrate the design and performance of the proposed controller which has been designed to make the grid side neutral current equal to zero.

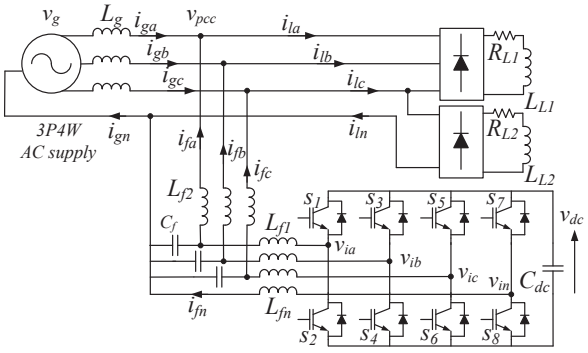

Fig. 1. Four-wire three-phase shunt active power filter

The nominal RMS voltage at the Point of Common Coupling (PCC) was set to 230 V (50 Hz). The DC voltage of the VSC was set to 500 V. The LCL filter consists of L_{f1} = L_{f2} = 1.5 mH and C_f = 20 μF. The grid inductance is L_g = 330 μH which results in a strong grid. The inductance at the neutral leg is L_{fn} = 4 mH. The grid X_s/R_s ratio has been set to 10. A 5 kVA unbalanced and non-linear load is connected to emulate the current harmonics consumption. The inverter switching frequency and the control sampling frequency were set to 5 kHz.

The zero-sequence state-space model of the plant is:

$$\frac{d\boldsymbol{x}_0}{dt} = \boldsymbol{A}_0 \cdot \boldsymbol{x}_0 + \boldsymbol{B}_{10} \cdot \boldsymbol{u}_{10} - \boldsymbol{B}_{20} \cdot \boldsymbol{u}_{20} \tag{1}$$

where the state-variable vector is $\boldsymbol{x}_0 = [i_{Lf10}\ v_{Cf0}\ i_{Lf20}]^t$, the input vector is $\boldsymbol{u}_{10} = [v_{i0}]$, the disturbance vector is $\boldsymbol{u}_{20} = [v_{pcc0}]$ and:

$$\boldsymbol{A}_0 = \begin{bmatrix} \frac{-R_{f1}-3R_{fn}}{L_{f1}+3L_{fn}} & \frac{-1}{L_{f1}+3L_{fn}} & 0 \\ \frac{1}{C_f} & 0 & \frac{-1}{C_f} \\ 0 & \frac{1}{L_{f2}} & \frac{-R_{f2}}{L_{f2}} \end{bmatrix} \tag{2}$$

$$\boldsymbol{B}_{10} = \begin{bmatrix} \frac{1}{L_{f1}+3L_{fn}} & 0 \\ 0 & \frac{1}{L_{f1}+3L_{fn}} \\ 0 & 0 \end{bmatrix} \quad \boldsymbol{B}_{20} = \begin{bmatrix} 0 & 0 \\ \frac{1}{L_{f2}} & 0 \\ 0 & \frac{1}{L_{f1}} \end{bmatrix} \tag{3}$$

The magnitude of the frequency response of the described plant transfer function $P_0(s) = I_{Lf20}(s)/V_{i0}(s)$ is drawn in Fig. 2 (solid line) showing an important resonance peak at f_{res} = 986 Hz.

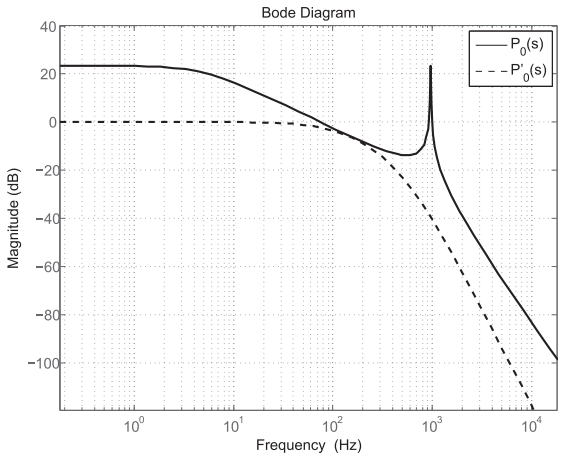

Fig. 2. Bode diagram of the open-loop and closed-loop frequency response of the zero-sequence model

III. Zero-Sequence Component Control in SRFS

The typical procedure to apply a SRF controller to the zero-sequence component of a four-wire three-phase converter (a single-phase system) is depicted in Fig. 3 [12]. A quadrature signal is created in order to have the two components of the $\alpha\beta$ rotating vector before it is referred to a dq synchronously-rotating frame. The main controller is used to damp the resonance of the filter and each SRF-based controller is used to track single-phase sinusoidal references of different frequencies.

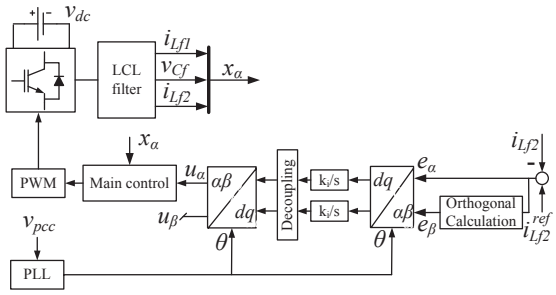

Fig. 3. Typical SRF-based controller scheme for single-phase systems

Assuming that the orthogonal signal e_β is generated correctly in Fig. 3, the equivalent $\alpha\beta$ frame representation of the controller is as shown in Fig. 4. The transformation from $\alpha\beta$ to dq uses:

$$\mathbf{R}(n\theta) = \begin{bmatrix} \cos(n\theta) & -\sin(n\theta) \\ \sin(n\theta) & \cos(n\theta) \end{bmatrix} \tag{4}$$

where n is the harmonic order and $\theta = \omega_g t$, which is provided by the PLL. The control signal u_α can be calculated as:

$$
\begin{aligned}
u_\alpha &= u'_d cos(n\theta) + u'_q sin(n\theta) \\
&= \left[k_i \int e'_d \, dt\right] \, cos(n\theta) + \left[k_i \int e'_q \, dt\right] \, sin(n\theta) \\
&= \left[k_i \int [e_\alpha cos(n\theta) - e_\beta sin(n\theta)] \, dt\right] cos(n\theta) + \\
&\quad \left[k_i \int [e_\alpha sin(n\theta) + e_\beta cos(n\theta)] \, dt\right] sin(n\theta)
\end{aligned} \tag{5}
$$

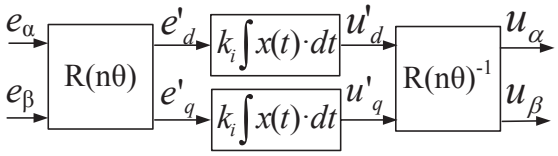

Fig. 4. Equivalent $\alpha\beta$ frame representation of the controller

Notice that he control signal u_α in (5) depends on both error signals e_α and e_β. Using the Laplace Transform on (5) yields:

$$
U_\alpha(s) = \frac{k_i s}{s^2 + (n\omega_g)^2} E_\alpha(s) + \frac{k_i n\omega_g}{s^2 + (n\omega_g)^2} E_\beta(s) \tag{6}
$$

which shows two resonant controllers. Therefore, the closed-loop system can track, with zero error, a sinusoidal signal with frequency equal to $n\omega_g$. However, there is a cross-coupling between $U_\alpha(s)$ and $E_\beta(s)$ which depends on the selection of $E_\beta(s)$ and it has to be taken into account. The quadrature signal of $E_\alpha(s)$ is required to have DC values at the input of the integrators (e'_d and e'_q).

A. Methods for the generation of a orthogonal signal

There are different methods in the literature to create the orthogonal signal from a single-phase signal. The simplest technique is to implement a phase lag of 90 degrees [15]. However, the dynamic performance deteriorates with this method because the controller cannot respond instantaneously to changes in the error.

Another approach is to use a derivative or an integral of the original signal. However, the derivative amplifies noise [16] whilst, with the integrator, the amplitude of the signal changes with frequency, complicating the design of the integrator gains for harmonic compensation. Kalman filters [17] and Hilbert Transformation [18] have also been proposed but they are complex techniques that require large computational effort.

Finally, an all-pass filter is implemented in [12] . This filter is tuned to produce a phase lag of 90 degrees at the targeted frequencies. However, a different filter is required for each harmonic and, during frequency variations, this filters should be adapted with a special focus on the stability.

B. Proposed method

Two rotations applied to the original zero-sequence component are proposed instead of using the quadrature signal.

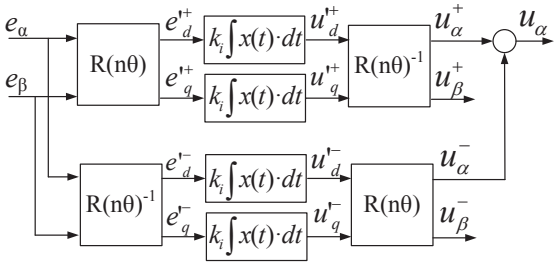

Fig. 5. Equivalent $\alpha\beta$ frame representation of the proposed controller

The angular speeds of these two rotations are equal but with opposite signs producing a positive and a negative sequence (see Fig. 5). Adding the contributions of the positive- and negative-sequence control signals (u^+_α and u^-_α, respectively) the total control signal u_α can be written as:

$$
\begin{aligned}
u_\alpha &= \left[k_i \int [e_\alpha cos(n\theta)] \, dt\right] cos(n\theta) \\
&+ \left[k_i \int [e_\alpha sin(n\theta)] \, dt\right] sin(n\theta)
\end{aligned} \tag{7}
$$

where the control signal u_α depends only on the error signal e_α. Laplace Transform on (7) yields:

$$
U_\alpha(s) = \frac{2k_i s}{s^2 + (n\omega_g)^2} E_\alpha(s) \tag{8}
$$

Consequently, the orthogonal signal of e_α (e_β) is not required now.

Fig. 6 shows the fundamentals of the proposed MSRF-based control scheme in dq for the zero-sequence component. The $sin(n\theta)$ and $cos(n\theta)$ in (4) are calculated with the $sin(\theta)$ and $cos(\theta)$ provided by the PLL and by using the DeMoivre's formula recursively [19]:

$$
cos(n\theta) + jsin(n\theta) = (cos(\theta) + jsin(\theta))^n \tag{9}
$$

as in the so-called "Efficient" Multiple Reference Frame (EMRF) controller proposed in [11]. As shown in [11], the stability margins of the closed-loop system can be improved by using a matrix containing the frequency response of the closed-loop system composed by the plant and the main controller evaluated at each targeted frequency:

$$
\mathbf{\Gamma}_n = \begin{bmatrix} a_n & -b_n \\ b_n & a_n \end{bmatrix} \tag{10}
$$

where a_n and b_n can be calculated as in [11].

The complete proposed scheme is shonw in Fig. 6. DeMoivre's formula is included in block "SRF generation". For simplicity, a pure integrator can be used in each SRF to control the zero-sequence component. Afterwards, the contributions of the control signal for the positive sequence and the one for the negative sequence are added. This method can be applied to all harmonic frequencies by using the corresponding frequency in each case. The procedure shows an intrinsic frequency adaptation capability because it updates the rotation matrices with the $sin(\theta)$ and $cos(\theta)$

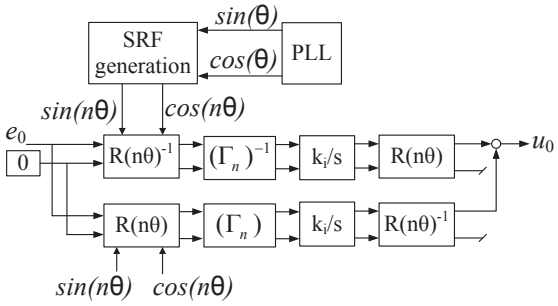

Fig. 6. Proposed zero-sequence controller scheme in dq

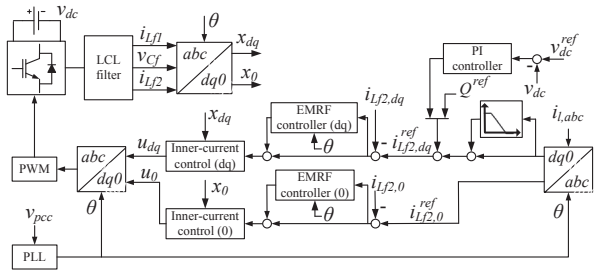

Fig. 7. Proposed control scheme for dq and zero-sequence components

values given by the PLL.

Following the Laplace Transform in [20], the equivalent transfer function in the stationary reference frame of the proposed method for one harmonic is:

$$C_n(s) = \frac{U_0(s)}{E_0(s)} = 2k_i \frac{(a_n s - b_n n\omega_g)}{s^2 + (n\omega_g)^2} \qquad (11)$$

Although the proposed method acts as a resonant controller for one component, it is implemented in multiple SRFs as in Fig. 6 to take advantage of its frequency adaptation capability. The equivalent resonant controller can be used to calculate the stability margins and to design the gain k_i of the pure integrator.

IV. Design of the Controllers in SRFs

The control scheme of the four-wire three-phase converter is depicted in Fig. 7 where the control of the output current of the filter is achieved by means of two controllers as described below.

A. Main-controller design

A state-feedback controller is used as the inner-current controller for the zero-sequence component. It places two dominant real poles at $-3 \times \omega_g$ and the remaining poles at $-30 \times \omega_g$, where ω_g is the grid frequency in rad/s. The magnitude of the frequency response of the closed-loop transfer function $P_0'(s)$ is depicted in Fig. 2 (dashed line) and it shows that the resonance has been suppressed. A similar state-feedback controller is used as the inner-current control for the dq components. This controller deals with the resonance and the cross-coupling between d and q axes (see [11] for details).

B. Harmonic-controller design

The placement of the EMRF controller is shown in Fig. 7. The unbalanced non-linear load depicted in Fig. 1, which is connected between one phase and the neutral point, produces odd harmonics in the zero-sequence component. Therefore, the EMRF controller for this component has to track harmonics $n = 1, 3, 5, ..., 31$.

The stability analysis cannot be carried out for each SRF independently. Accordingly, the equivalent resonant controller in (11) is used to calculate the open-loop frequency response required to analyse the stability. The block diagram used for the stability analysis is depicted in Fig. 8. The frequency response of the open-loop transfer function $G_0(s) = -U_0'(s)/U_0(s)$, which includes the equivalent resonant controllers, has been drawn in Fig. 9, for the case study. The same value of k_i is used for all harmonics.

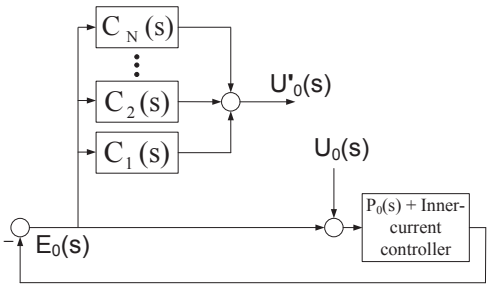

Fig. 8. Open-loop block diagram for stability analysis

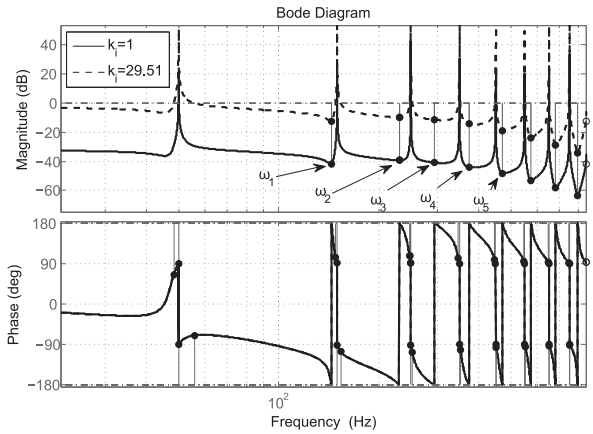

Fig. 9. Open-loop frequency response with different values of k_i.

Two different values of k_i have been used in Fig. 9. The phase margins are always close to 90^o thanks to the use of the inverse frequency response (Γ_n). Varying k_i will not change much these phase margins because of the sharp magnitude changes shown in the upper plot of Fig. 9. The design of k_i will mainly affect the gain margins which have to be evaluated at the ultimate frequencies ω_h. Which one of the gain margins is most critical depends on the design of the main controller. The value of k_i finally implemented in the prototype ($k_i = 29.51$) gives a minimum gain margin of

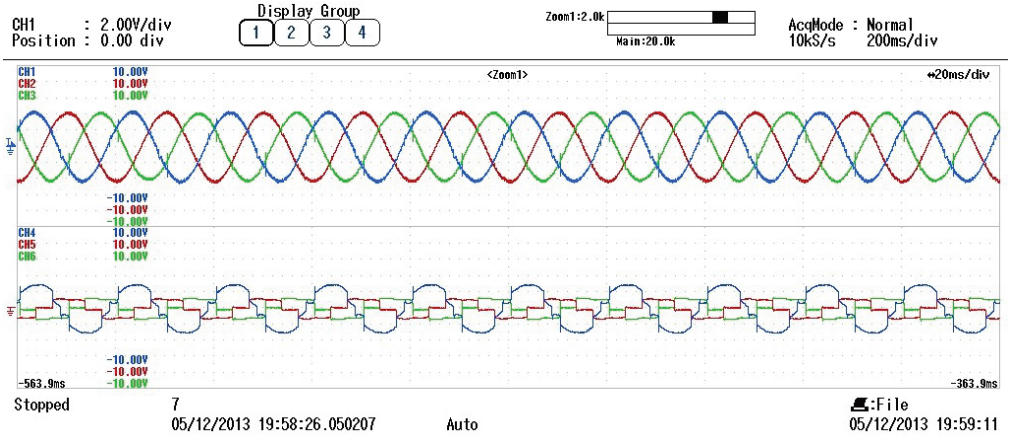

Fig. 10. Grid (top plot) and load (bottom plot) currents in steady state with the EMRF controller enabled

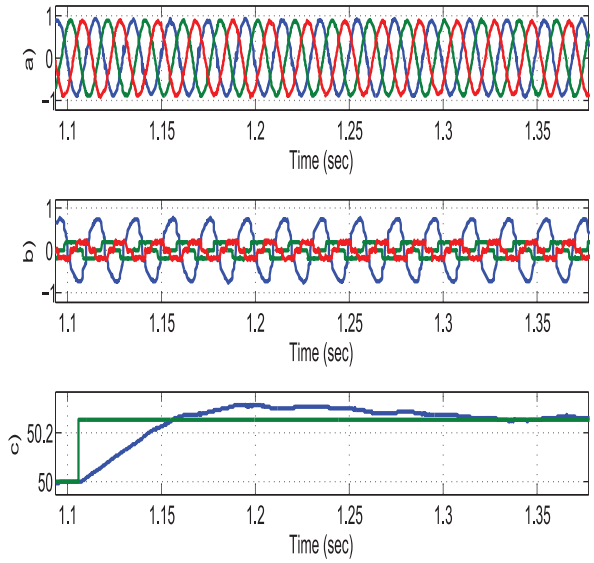

Fig. 11. Transient response of the three-phase grid currents during a grid frequency variation: a) grid currents, b) load currents and c) grid frequency

10 dB. Finally, the EMRF controller for the dq components is designed as in [11].

C. DC voltage control

A DC voltage controller is used to keep the DC bus of the converter constant to ensure the correct operation during the harmonic compensation. The DC voltage is controlled by changing the DC valude of the d component of the filter-current set point in the main SRF. A PI controller is used for this purpose with gains $k_{pdc} = 2$ and $k_{idc} = 10$.

V. Experimental results

A prototype as shown in Fig. 1 has been build to illustrate the EMRF controller performance. The full control algorithm is implemented in Matlab/Simulink and it is downloaded into a dSpace 1103 platform. The VSC is a Semikron SKS 22F B6U.

The plant model for the frequencies of interest is identified at the beginning of the experiment, just after the main controller is activated. After 500 ms, the frequency response for each harmonic is automatically obtained and, then, the inverse of Γ_n is calculated once. In the EMRF controller for the dq components, $k_i = 10$ while $k_i = 2$ for the zero-sequence EMRF controller.

The harmonic controller for the dq components has been set to tackle even harmonics from the 2nd to the 30th. The harmonic controller for the zero-sequence component has been set to tackle odd harmonics from the 1st to the 31st. The three-phase grid and load currents in steady state are shown in Fig. 10. The resultant THDs of the load and grid currents are: phase A (28.79% and 1.36%, respectively), phase B (29.26% and 1.66%, respectively) and phase C (17.5% and 2.33%, respectively). Clearly, the three-phase grid current is now balanced and, consequently, the current through the neutral wire is zero.

Fig. 11 illustrates the performance of the proposed controller when there is a 0.25 Hz step change in the grid frequency which is estimated by a PLL and used to update the harmonic controllers. The grid-current harmonics for the dq components when the grid frequency changes can be seen in Fig. 12 and, for the zero-sequence component, harmonics can be seen in Fig. 13. Fig. 12 and Fig. 13 show that the harmonics and the imbalance in the grid currents are suppressed, even under grid frequency variations.

VI. Summary and conclusions

This paper proposes the use of an efficient multiple-reference-frame (EMRF) controller for harmonic control in four-wire, three-phase custom power devices, as an alternative to orthogonal-signal generation methods. This method is expected to show better dynamic performance than those relaying on the generation of an orthogonal signal, since

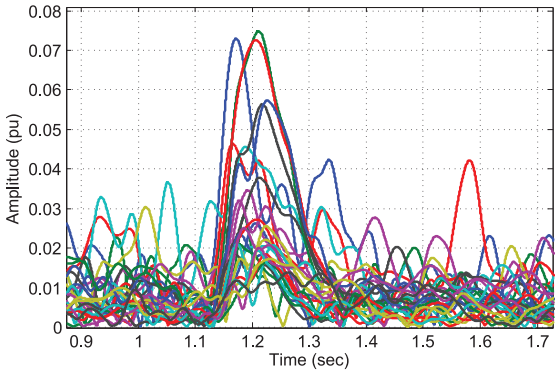

Fig. 12. Harmonic level of the dq components of the grid currents during a grid frequency variation

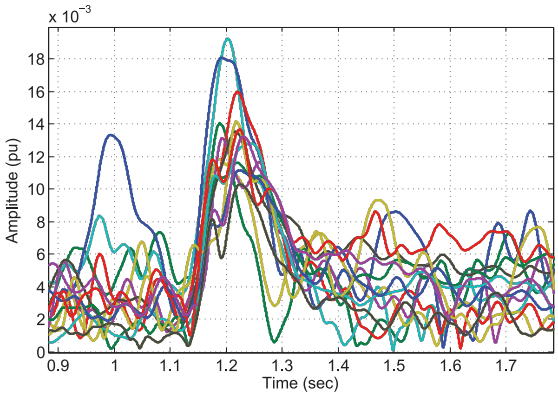

Fig. 13. Harmonic level of the zero-sequence component of the grid currents during a grid frequency variation

no additional dynamics are introduced in the calculations. Pure integrators applied on each SRF can be used to tackle each harmonic whilst the computation effort is maintained reasonably low.

The frequency response of the plant at the harmonic frequencies was used for compensation in a plug-in structure of the controller making it possible to use the same gain k_i for all harmonics. Therefore, the design of the EMRF controller is independent of the number of harmonics. However, if required, special attention can be given to any of the harmonics to be tackled.

Grid-frequency adaptation is implemented naturally and harmonic control can respond very quickly to this variation. Experimental results of a four-wire, three-phase shunt active power compensator show, not only the effectiveness of the proposed control system, but also the simple methodology for the stability analysis and the design.

Acknowledgements

The Spanish Government (project ENE2011-28527-C04-01 and BES-2012-055790) has partially financed this work.

References

[1] T.M. Gruzs. A survey of neutral currents in three-phase computer power systems. *Industry Applications, IEEE Transactions on*, 26(4):719–725, 1990.

[2] Yi Tang, Poh Chiang Loh, Peng Wang, Fook Hoong Choo, Feng Gao, and Frede Blaabjerg. Generalized design of high performance shunt active power filter with output LCL filter. *IEEE Transactions on Industrial Electronics*, 59(3):1443–1452, March 2012.

[3] V. Blasko, L. Arnedo, P. Kshirsagar, and S. Dwari. Control and elimination of sinusoidal harmonics in power electronics equipment: A system approach. In *Energy Conversion Congress and Exposition (ECCE), 2011 IEEE*, pages 2827–2837, 2011.

[4] D.N. Zmood and D.G. Holmes. Stationary frame current regulation of PWM inverters with zero steady-state error. *IEEE Transactions on Power Electronics*, 18(3):814–822, May 2003.

[5] X. Yuan, W. Merk, H. Stemmler, and J. Allmeling. Stationary frame generalized integrators for current control of active power filters with zero steady state error for current harmonics of concern under unbalanced and distorted operation conditions. *IEEE Transactions on Industry Applications*, 38(2):523–532, March/April 2002.

[6] Marten F. Byl, Stephen J. Ludwick, and David L. Trumper. A loop shaping perspective for tuning controllers with adaptive feedforward cancellation. *Precision Engineering*, 29(1):27–40, January 2005.

[7] Shane Malo and Robert Grin. Adaptive feed-forward cancellation control of a full-bridge dc-ac voltage inverter. In *The International Federation of Automatic Control. Proceedings of the 17th World Congress*, pages 4571–4576, 2008.

[8] A. García-Cerrada, O. Pinzón-Ardila, V. Feliu-Batlle, P. Roncero-Sánchez, and P. Garcia-González. Application of a repetitive controller for a Three-Phase active power filter. *IEEE Transactions on Power Electronics*, 22(1):237–246, January 2007.

[9] J. Roldán-Pérez, A. García-Cerrada, J.L. Zamora-Macho, Roncero-Sánchez P., and E. Acha. Troubleshooting a digital repetitive controller for a versatile dynamic voltage restorer. *International Journal of Electrical Power and Energy Systems*, 57:105–115, 2014.

[10] S.J. Lee and S.-K. Sul. A harmonic reference frame based current controller for active filter. In *Proc. Applied Power Electronics Conference (APEC)*, pages 1073–1078, 2000.

[11] M. Ochoa-Gimenez, J. Roldan-Perez, A. Garcia-Cerrada, and J.L. Zamora-Macho. Space-vector-based controller for current-harmonic suppression with a shunt active power filter. In *Power Electronics and Applications (EPE), 2013 15th European Conference on*, pages 1–10, 2013.

[12] M. Monfared, S. Golestan, and J.M. Guerrero. Analysis, design, and experimental verification of a synchronous reference frame voltage control for single-phase inverters. *IEEE Transactions on Industrial Electronics*, 61(1):258–269, January 2014.

[13] N. Soni, S. Doolla, and M. C. Chandorkar. Improvement of transient response in microgrids using virtual inertia. *IEEE Transactions on Power Delivery*, 28(3):1830–1838, July 2013.

[14] S. Mishra, G. Mallesham, and A.N. Jha. Design of controller and communication for frequency regulation of a smart microgrid. *IET Renewable Power Generation*, 6(4):248–258, 2012.

[15] R. Zhang, M. Cardinal, P. Szczesny, and M. Dame. A grid simulator with control of single-phase power converters in d-q rotating frame. In *Power Electronics Specialists Conference, 2002. pesc 02. 2002 IEEE 33rd Annual*, volume 3, pages 1431–1436 vol.3, 2002.

[16] A. Roshan, R. Burgos, A.C. Baisden, F. Wang, and D. Boroyevich. A d-q frame controller for a full-bridge single phase inverter used in small distributed power generation systems. In *APEC 2007 - Twenty Second Annual IEEE Applied Power Electronics Conference*, pages 641–647, February 2007.

[17] K. De Brabandere, T. Loix, K. Engelen, B. Bolsens, J. Van den Keybus, J. Driesen, and R. Belmans. Design and operation of a phase-locked loop with kalman estimator-based filter for single-phase applications. In *IECON 2006 - 32nd Annual Conference on IEEE Industrial Electronics*, pages 525–530, November 2006.

[18] M. Saitou and T. Shimizu. Generalized theory of instantaneous active and reactive powers in single-phase circuits based on hilbert transform. In *Power Electronics Specialists Conference, 2002. pesc 02. 2002 IEEE 33rd Annual*, volume 3, pages 1419–1424 vol.3, 2002.

[19] M. Hazewinkel, editor. *Encyclopedia of Mathematics*. Springer, 2001.

[20] D.N. Zmood, D.G. Holmes, and G.H. Bode. Frequency-domain analysis of three-phase linear current regulators. *IEEE Transactions on Industry Applications*, 37(2):601–610, March/April 2001.